PHYSICAL REVIEW LETTERS

Experimental Realization of an On-Chip All-Optical Analogue to Electromagnetically Induced Transparency

Qianfan Xu,[1] Sunil Sandhu,[2] Michelle L. Povinelli,[2] Jagat Shakya,[1] Shanhui Fan,[2] and Michal Lipson[1,*]

[1]*School of Electrical and Computer Engineering, Cornell University, Ithaca, New York 14853, USA*
[2]*Department of Electrical Engineering, Stanford University, Stanford, California 94305, USA*
(Received 21 December 2005; published 27 March 2006)

We provide the first experimental observation of structure tuning of the electromagnetically induced transparencylike spectrum in integrated on-chip optical resonator systems. The system consists of coupled silicon ring resonators with 10 μm diameter on silicon, where the coherent interference between the two coupled resonators is tuned. We measured a transparency-resonance mode with a quality factor of 11 800.

Recent theoretical analysis of coupled microresonators has revealed that coherent effects in coupled resonator systems are remarkably similar to those in atoms [1–8]. Similar to the atomic systems, where electromagnetically induced transparency (EIT) occurs due to quantum interference effects induced by coherently driving the atom with an external laser [9,10], induced transparency can also occur in a photonic resonator system where coherent interference between two coupled resonators is instead enforced by the geometry of a nanophotonic structure [3,5]. In systems like the one demonstrated in [1], the Q of the system is limited by the higher-Q resonator, determined by the weak but nonzero coupling to the adjacent waveguide as well as the loss due to scattering. In [6] it was pointed out that for particular configurations of waveguides side coupled to resonators, there exists an all-optical dark state that can be asymptotically decoupled from the waveguide for proper tuning of the resonator frequencies. In such a case the Q of the system is limited only by the scattering losses of the system. The existence of such an all-optical dark state, which gives rise to an EIT-like transmission spectrum, is critical for on-chip coherent manipulation of light at room temperatures, including the capabilities of stopping, storing, and time reversing an incident pulse [6]. The observation of an EIT-like spectrum in a resonator system was reported in [11] in a compound glass waveguide platform using relatively large resonators. Here, we provide the first experimental observation of structural tuning of the EIT-like spectrum in integrated micron-size silicon optical resonator systems. Our results demonstrate that the resonant interference required for coherent manipulation of light can indeed be achieved on-chip without the use of atomic resonance. Consequently, many of the basic limitations on bandwidth and decoherence that result from the fragility of the electronic coherence may be fundamentally overcome. This work therefore has broad implications for optical communications and quantum information processing.

A top-down microscope image of our experimental system is shown in Fig. 1. The system consists of a pair of microring resonators coupled to parallel waveguides. Input power enters the bottom waveguide in the direction labeled "IN," and transmitted power is measured farther along the waveguide in the direction labeled $|T(\lambda)|^2$. Properly designed, the system can exhibit an EIT-like transmission spectrum: a narrow transparency peak in the center of a broader transmission dip [4,11,12]. The characteristic shape of the spectrum can be understood by first considering the effect of a single-ring resonator between parallel waveguides. A single-ring transmission spectrum exhibits a dip at the resonant wavelength of the ring, due to coupling of input light into the counterclockwise mode of the ring and back out into the left-going mode of the upper waveguide. For brevity, we term this process "reflection," since the output light, labeled as $|R(\lambda)|^2$, exits in the opposite direction it entered. Putting two rings together allows a resonance to form via multiple, constructively interfering "reflections" between the rings, which we will call a "transparency resonance." By adjusting the separation between the rings, the transparency resonance can be made to coincide with the resonant wavelength of the rings. The spectrum will then exhibit a narrow transparency peak in the center of a broader transmission dip; this is the EIT-like transmission spectrum. In practice, a slight nonzero detuning of the two ring resonances is preferred to prevent the degradation of the transparency peak in the presence of loss.

Our device is fabricated on a silicon-on-insulator substrate with a 3 μm-thick buried oxide layer. The wave-
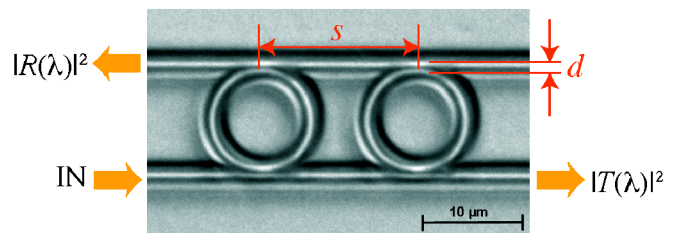

FIG. 1 (color online). Microscope picture of the fabricated microring-resonator system.

guides and rings are defined using electron-beam lithography followed by reactive ion plasma etching. The resulting structure is covered by 3 μm-thick SiO_2 upper cladding deposited by plasma-enhanced chemical vapor deposition [13], yielding silicon waveguides and rings surrounded on all sides by oxide. Both the straight waveguides and the waveguides forming the rings have a width of 450 nm and a height of 250 nm. Nanotapers are used at both ends of the input waveguide to ensure low-loss coupling between optical fiber and waveguide. The center-to-center (CTC) distance between the straight waveguide and the rings (d) is 610 nm, and the CTC distance between the rings (s) is 15.69 μm. The diameters of the rings are 10 μm, where a slight difference in perimeter between the two rings (8 nm) is introduced to detune the ring resonances by $\sim$0.4 nm. The transmission spectra of the device are measured using a tunable laser. At the input side, light from the tunable laser is coupled through a tapered lensed fiber to the nanotaper. At the output side, light is collimated using a lens and sent to a detector through a polarizer. Figure 2(a) shows the normalized power transmission spectrum for the quasi-TM mode (dominant electric field perpendicular to the substrate) of the device. The characteristic EIT-like line shape is apparent. The FWHM of the transparency peak is $\sim$0.13 nm, corresponding to a quality factor of $Q_{tr} =$ 11 800. The quality factor of the transparency resonance Q_{tr} is much higher than the loaded quality factor of each individual ring resonator [4], which is $\sim$1000 as will be shown later. For the quasi-TE mode, the detuning between the two ring resonances is larger than the width of each individual ring resonance ($\sim$0.15 nm); therefore the EIT-like spectrum is not observed.

To test the dependence of the transparency resonance on the separation between the rings, additional devices with varying separations s from 15.71 to 15.77 μm were fabricated and measured. The black, solid curves labeled (b) through (e) in Fig. 2 show the transmission spectra. For clarity, each successive curve is offset by -0.5 units. Because of slight variations in fabrication, the center wavelength of the overall line shape shifts slightly ($< \pm 1$ nm). From the figure, it is seen that devices with increased values of s exhibit less symmetric line shapes with significantly broader central peaks. The pronounced narrowing of the central peak for the optimum ring separation of curve (a) provides strong indication of the coherent, resonant interaction between the two rings. Moreover, we directly imaged the optical mode at the transparency-resonance wavelength by collecting the top-scattered light from the optimal device, as shown in Fig. 3. One can clearly see the strong optical excitation of both rings, as well as constructive interference in the waveguide regions between the rings. Note that the waveguide on the upper right side is illuminated by a strong scattering point on the ring resonator close by. Light does not propagate through that waveguide.
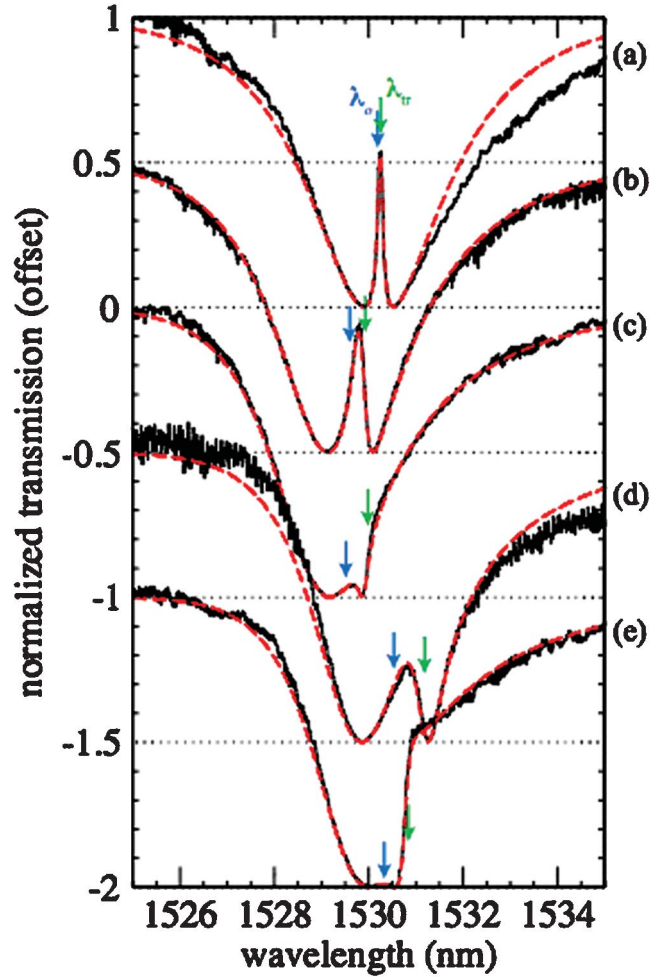

FIG. 2 (color). Experimental transmission spectra (black, solid line) and theoretical fits (red, dashed line) for the microring-resonator system of Fig. 1. Curves (a)–(e) correspond to five different devices with varying ring separations s. Successive curves have been offset by -0.5 units for clarity. (a) $s =$ 15.69 μm. (b) $s = 15.71$ μm. (c) $s = 15.73$ μm. (d) $s = 15.75$ μm. (e) $s = 15.77$ μm.

The experimental transmission spectra are well explained by a theoretical model. The power transmission [4] can be written as

$$|T(\lambda)|^2 = \left(\frac{|t_A t_B|}{1 - |r_A r_B|}\right)^2 \frac{1}{1 + 4(\frac{\sqrt{|r_A r_B|}}{1-|r_A r_B|})^2 \sin^2\theta}, \quad (1)$$

where t_A and t_B are complex transmission coefficients for resonator A and B respectively, given by

$$t_{A,B} = \frac{j(\omega - \omega_{A,B}) + \gamma}{j(\omega - \omega_{A,B}) + (\gamma_c + \gamma)}, \quad (2)$$

where $\omega_{A,B}$ is the resonant frequency of resonator A or B; $\omega = 2\pi c/\lambda$. γ is the amplitude radiative-loss rate, related to the radiative quality factor as $\gamma = \pi c/Q_{rad}\lambda_0$. γ_c is the total waveguide-ring amplitude-coupling rate due to decay

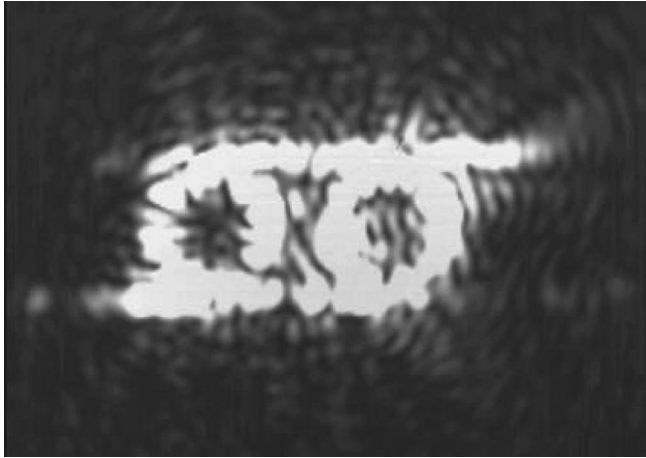FIG. 3. Optical mode at the EIT-like transparency-resonance imaged by collecting the top-scattered light at the transparency peak λ_{tr}.

into both lower and upper waveguides; $\gamma_c = \pi c/Q_c\lambda_0$. r_A and r_B are the complex reflection coefficients, given by

$$r_{A,B} = \frac{\gamma_c}{j(\omega - \omega_{A,B}) + (\gamma_c + \gamma)}. \qquad (3)$$

θ is one-half the round-trip phase accumulated in the waveguides: $\theta = \frac{1}{2}\mathrm{Arg}[r_A r_B e^{-2j\beta(\omega)s}]$, where $\beta(\omega)$ is the waveguide dispersion relationship. Equation (1) has the form of transmission through a Fabry-Perot cavity [14], but with frequency-dependent, resonant mirrors whose transmission and reflection coefficients are given by Eqs. (2) and (3).

The red, dashed lines in Figs. 2(a)–2(e) show the theoretical fits. The waveguide dispersion relation was obtained by direct numerical solution [15], using the experimental dimensions of the waveguide cross section, a refractive index of 3.45 for silicon, and a refractive index of 1.46 for the silicon oxide cladding: $\beta(\omega) = 1.4 \times 10^{-17}\,\mathrm{nm}^{-1}\mathrm{s}\ \omega - 8.9 \times 10^{-3}\,\mathrm{nm}^{-1}$. The ring resonance wavelengths λ_A and λ_B were found from the minima of the transmission spectra. The remaining parameters were fit in the following manner. Q_c was adjusted (between 975 and 1025) to fit the background shape of the wide transmission dip. The nominal length $s(= 15.7\ \mu\mathrm{m})$ was tuned by a small amount Δs (between 0.09 and 0.10 μm) to obtain the right shape of the narrow, central peak, and last, Q_{rad} was adjusted (between 25 000 and 35 000) to fit the amplitude of the center peak.

To systematically understand the trends shown in Fig. 2, we write the transmission as a product of two terms: $|T(\lambda)|^2 = P_{max}(\lambda)H(\lambda)$, where $P_{max} \equiv [|t_A t_B|/(1 - |r_A r_B|)]^2$ and $H(\lambda) \equiv 1/[1 + 4[\sqrt{|r_A r_B|}/(1 - |r_A r_B|)]^2\sin^2\theta]$. P_{max} represents the maximum possible transmitted power through the waveguide-resonator system. For a Fabry-Perot cavity, this quantity would be independent of wavelength. For our system, it exhibits

dips at the resonance wavelengths of the rings and a local maximum at the center wavelength λ_0. H determines the wavelength of the transparency resonance (λ_{tr}). Similar to a Fabry-Perot cavity, H is maximized when the round-trip phase (2θ) is a multiple of 2π. When λ_{tr} and λ_0 coincide, the resulting transmission spectrum exhibits a narrow, symmetric peak. As the two wavelengths shift away from each other, broadened, asymmetric line shapes are observed. This trend is seen in Fig. 2, where λ_0 and λ_{tr} are indicated by blue and green arrows, respectively. We note that curve (d) exhibits a sizeable central peak height despite a relatively large misalignment between λ_0 and λ_{tr}; this is due to the comparatively large detuning of the two ring resonances in this particular device. Overall, the loss of the EIT-like line shape as the two wavelengths separate provides direct experimental evidence of coherent interactions between the rings.

In conclusion we show experimentally the existence of a dark state with an EIT-like properties in an on-chip device. The observed effect precisely demonstrates the required interference scheme that satisfies the optimal conditions for on-chip all-optical slowing and stopping of light [6]. In addition, the capability for creating such transparency resonance, and for controlling the linewidth of such resonance through tuning, is important for applications such as tunable bandwidth filter, as well as for switching and nonlinear optics applications. By tuning the resonator system, the system would enable applications for on-chip optical interconnects and optical processing, where light storage and nonlinear components [16] could be achieved using micron-sized integrated silicon devices [17].

*Electronic address: lipson@ece.cornell.edu
[1] D. D. Smith, H. Chang, K. A. Fuller, A. T. Rosenberger, and R. W. Boyd, Phys. Rev. A **69**, 063804 (2004).
[2] J. B. Khurgin, J. Opt. Soc. Am. B **22**, 1062 (2005).
[3] W. Suh, Z. Wang, and S. Fan, IEEE J. Quantum Electron. **40**, 1511 (2004).
[4] L. Maleki, A. B. Matsko, A. A. Savchenkov, and V. S. Ilchenko, Opt. Lett. **29**, 626 (2004).
[5] A. B. Matsko, A. A. Savchenkov, D. Strekalov, V. S. Ilchenko, and L. Maleki, J. Mod. Opt. **51**, 2515 (2004).
[6] M. F. Yanik, W. Suh, Z. Wang, and S. Fan, Phys. Rev. Lett. **93**, 233903 (2004).
[7] A. Naweed, G. Farca, S. I. Shopova, and A. T. Rosenberger, Phys. Rev. A **71**, 043804 (2005).
[8] J. B. Khurgin, Phys. Rev. A **62**, 013821 (2000).
[9] S. E. Harris, Phys. Today **50**, No. 7, 36 (1997).
[10] M. D. Lukin and A. Imamoglu, Nature (London) **413**, 273 (2001).

[11] S. T. Chu, B. E. Little, W. Pan, T. Kaneko, and Y. Kokebun, IEEE Photonics Technol. Lett. **11**, 1426 (1999).

[12] A. Melloni, Opt. Lett. **26**, 917 (2001).

[13] V. R. Almeida, C. A. Barrios, R. R. Panepucci, and M. Lipson, Nature (London) **431**, 1081 (2004).

[14] B. E. A. Saleh and M. C. Teich, *Fundamentals of Photonics* (Wiley, New York, 1991), Chap. 9.

[15] S. G. Johnson and J. D. Joannopoulos, Opt. Express **8**, 173 (2001).

[16] V. Van, T. A. Ibrahim, P. P. Absil, F. G. Johnson, R. Grover, and P.-T. Ho, IEEE J. Sel. Top. Quantum Electron. **8**, 705 (2002).

[17] K. Wada, H. C. Luan, D. R. C. Lim, and L. C. Kimerling, Proc. SPIE-Int. Soc. Opt. Eng. **4870**, 437 (2002).